

# Design and simulation of FBAR with different electrodes material configuration

Yatin Kumar<sup>#1</sup>, Kamaljit Rangra<sup>\*2</sup>, Ravinder Agarwal<sup>#3</sup>

<sup>#</sup>M.E Dept of EIED, Thapar University, Patiala, India

<sup>#</sup>Professor Dept of EIED, Thapar University, Patiala, India

<sup>\*</sup>Chief scientist CSIR-CEERI, Pilani, India

**Abstract**— Thin film bulk acoustic resonator (FBAR) with high operating frequencies and the higher quality factor are preferred for many sensing applications. This paper presents FBAR device geometry for the different electrodes material optimize for the frequency range of 2.17 GHz to 4.49 GHz with the thickness of 1  $\mu\text{m}$  of the Aluminum nitrite (AlN) as a piezoelectric layer. The effective couplings of range 5.88% to 6.89% have been achieved. The quality factor for the different electrode materials varies from 360 to 820 for the same boundary conditions. Aluminum electrodes results in higher operating frequency as compared to platinum and tungsten. However, use of Al electrodes leads to lower coupling coefficient and quality factor as compared to platinum and tungsten. The equivalent Butterworth Van-Dyke (BVD) electrical parameters are also extracted. FBAR's flexibility of operating frequency, coupling coefficient and quality factor are achieved by different electrode configuration.

**Keywords**— Film Bulk Acoustic Resonator (FBAR), Quality Factor (Q), Coupling coefficient, CoventorWare, Aluminum Nitrite, Butterworth Van-Dyke (BVD)

## I. INTRODUCTION

In the last decade, a rapid growth has been identified in the thin film bulk acoustic resonator (FBAR) for sensing application and the wireless communication as filter and duplexers<sup>1</sup>. The first FBAR, presented in 1980 was having working frequency about 200 MHz<sup>2</sup>. In 1982, Lakin et al. demonstrated the potential of BAW device for filter and resonator<sup>3</sup>. A vast development in FBAR communication as duplexer achieved and first handset was presented in 2001<sup>4</sup>. A numerous applications of FBAR were developed as humidity sensor<sup>5</sup>, UV sensor<sup>6</sup>, DNA and protein detection<sup>7</sup>, microfluidics system<sup>8</sup>, mass sensor<sup>9</sup> and so on. FBAR has a thin film of piezoelectric layer sandwiched between the 2 electrodes. When a varying electric field applied, the piezoelectric layer starts to deform and deformation propagates through the bulk material FBAR in comparison to the surface acoustic wave (SAW) devices utilize bulk acoustic waves. FBAR has features like high power handling capacity, smaller size, high electrostatic discharge (ESD) because of the utilization of bulk of the device and also it has possibility of

integration with the CMOS technology. FBAR acts as an acoustic cavity resonator in which the acoustic waves bouncing back and forth between the walls, which are separated by a width of  $\lambda/2$  of the signal.

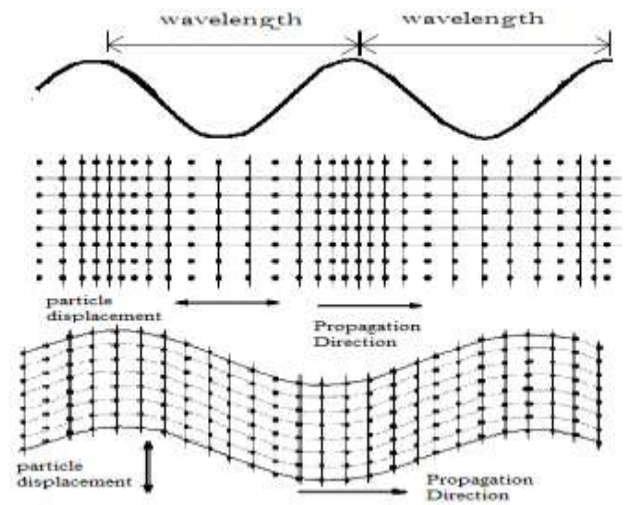


Figure 1 Longitudinal and transverse wave propagation

Piezoelectricity is a direct electrical-mechanical conversion occurring in certain type of crystal, which has discovered by Curie-brothers in 1880<sup>10</sup>. The piezoelectric thin films materials used in device are ZnO and AlN.

Table I Piezoelectric material properties

Material	AlN	ZnO	PZT	Units
Acoustic velocity	11.0	6.35	4.6	$10^3\text{m/s}$
Young's modulus	3.94	2.11	0.49	$10^{11}\text{N/m}^2$
Piezoelectric coeff. ( $d_{33}$ )	5.6	12.4	200	$10^{-12}\text{C/N}$
$k_{eff}^2$	6.5	8.5	35	%
Thermal conductance	320	60	1.8	W/mK
TCF	-25	-60	-	Ppm/

				°C
Dielectric constant	8.5-9.5	9.2	80-400	
Insertion loss	Very low	Low	high	

Both are wide band gap semiconductor. But AlN piezoelectric layer is used because it has superior material properties such as high acoustic velocity nearly 11000 m/s which is almost double of the ZnO. AlN has low dielectric losses and the lower temperature coefficient of frequency as shown in table I. AlN has a good thermal conductance so less heating issues. The coupling coefficient of PZT is much higher but the losses are very high and so it is not favorable for the device.

Table II Acoustic properties of various electrode materials

Material	Density (g/cm <sup>3</sup> )	Sonic velocity (10 <sup>3</sup> m/s)	Acoustic impedance	Thermal expansion (ppm)
Pt	21.5	3.96	8.474	8.9
Al	2.7	6.3	1.7	22.9
Mo	10.2	6.2	6.4	5.1
W	19.2	5.2	10	4.3

Table II shows the electrode materials properties. Aluminum is a good conductor and very easily available but has very low acoustic impedance and high thermal expansion. Platinum and tungsten has very high acoustic impedance as it is denser and withstand with high oxidation. Both have the lower thermal expansion. Molybdenum has the intermediate properties to the aluminum and platinum such as density and acoustic impedance. Molybdenum has good sonic velocity and very low thermal expansion.

The acoustic waves that propagate in FBAR are thickness excited waves which is parallel to the applied electric field as shown in figure (1). Lateral waves are also present, which propagate perpendicular to the electric field. Because FBAR utilize thickness excited waves for their operations, the lateral waves are undesirable and generates spurious modes. The Butterworth Van- dyke model<sup>11</sup> has been used for the electrical analysis of FBAR. The fabrication methods for FBAR are suggested as: back side wet etching<sup>12</sup> and front side surface etching.

In this paper, the FBAR has simulated for the different electrode materials having the thickness of 150 nm and the piezoelectric layer (AlN) of thickness 1µm. The simulation has been carried out and results are compared for frequencies, quality factors, coupling coefficients and impedances.

## II. DESIGN

Figure (2) shows the side view of the FBAR with different layers. It consists of silicon (100) as a substrate and a layer of thermally grown silicon oxide. Silicon oxide carries the device as a support layer, which has the AlN layer sandwiched between the electrodes. The FBAR needs the acoustic impedances mismatch to resonate properly and to achieve this, several methods of surface and bulk micromachining are suggested.

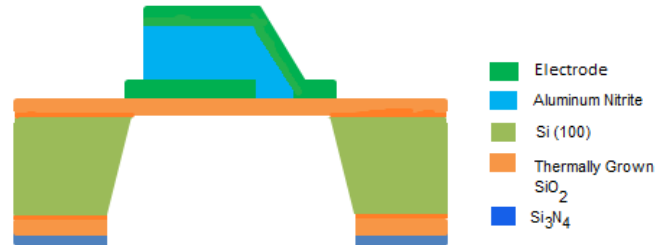


Figure 2 FBAR design

FBAR resonates at a particular frequency (equation 1) where the maximum energy has confined in the device.

$$f = \frac{v}{2d} \tag{1}$$

where v is acoustic velocity in piezoelectric layer and '2d' is the thickness of piezoelectric layer. This fundamental resonant frequency is observed when thickness is half the integral multiple of signal wavelength. FBAR uses the piezoelectric and inverse piezoelectric effect. The time varying electric signal is applied through the upper electrode then stress is generated (piezoelectric effect), which propagates in longitudinal direction in the crystal as acoustic waves as shown in figure 1. The acoustic waves reach the bottom electrode with a velocity given in the equation 2.

$$v_a = \sqrt{\frac{c}{\rho}} \tag{2}$$

where c is the stiffness and ρ is the density are the material properties. The quality factor is defined as the total energy confined in the device to the losses per cycle. In order to confine the energy in the device, the acoustic impedance of the electrodes and piezoelectric layer must be high. So the acoustic mismatch is increased at the interface and energy leakage is reduced. The quality factor for the FBAR is calculated as ratio of kinetic and potential energy in the device to the damping losses of the system and is given by

$$Q = \frac{v_a^2 \rho}{\omega \eta} \tag{3}$$

where  $\eta$  is the viscous damping coefficient.

A simple structure given by figure (2) is considered for the impedance calculation of the device by correlating the stress and electric field. The impedance is obtained as shown in equation 4.

$$Z = \frac{V}{I} = \frac{1}{j\omega C_0} \left[ 1 - K_t^2 \frac{\tan(kd)}{kd} \right] \tag{4}$$

where  $V$  is voltage,  $I$  is current,  $C_0$  is the capacitance of FBAR configuration,  $K_t^2$  is the coupling coefficient of material,  $k$  is the wave number and  $d$  is the thickness of piezoelectric layer. Impedance at resonance and anti-resonant frequency is zero and infinite respectively so the frequencies can be easily calculated and given by

$$\omega_a = (2n + 1) \frac{\pi v^D}{2 d} \tag{5}$$

$$\omega_r = \frac{v_a}{2d} \sqrt{1 - 8K_t^2 \frac{1}{2}} \tag{6}$$

where  $\omega_r$  and  $\omega_a$  are the resonant and anti resonant frequency. Coupling coefficient gives the efficiency of the energy conversion from electrical to mechanical domain and vice-versa. The coupling coefficient of the materials and the device are different. In the first case, material coupling coefficient shows that material is intrinsically better for making the electro-acoustic conversion than other materials. While in second case, device coupling coefficient is the combined influence of layers. Effective coupling is formulated as in terms of frequencies as:

$$K_{eff}^2 = \frac{\frac{\pi f_s}{2 f_p}}{\tan\left(\frac{\pi f_s}{2 f_p}\right)} \tag{7}$$

This equation can further simplifies as

$$K_{eff}^2 = \frac{\pi^2 f_s}{4 f_p} \left( \frac{f_p - f_s}{f_p} \right) \tag{8}$$

Quality factor and coupling coefficient of a device are inversely related to each other. For a device, both needs to be optimize and shown by constant called Figure of merit (FOM).

$$FOM(f) = k_{eff}^2 * Q(f) \tag{9}$$

FBAR's equivalent electrical model is presented by the Butterworth Van-Dyke (BVD) model. The equivalent circuit of BVD is shown in the figure 3.

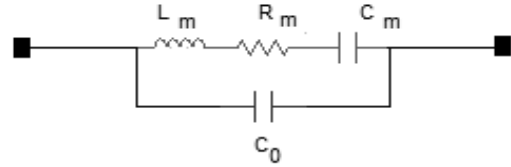


Figure 3 BVD model

The different component are assigned as

- Vibrating mass (motional inductor),  $L_m$
- Elasticity of piezoelectric material,  $C_m$
- Mechanical losses,  $R_m$
- Electrode form a static parallel plate capacitance,  $C_0$

$$f_s = \frac{1}{\sqrt{L_m \cdot C_m}} \tag{10}$$

$$f_p = f_s \left( 1 + \frac{C_m}{C_0} \right) \tag{11}$$

The resonant and anti-resonant frequencies of FBAR from the electrical model (BVD) can be calculated as shown in equation 10 and 11.

Figure of merit can be given in the terms of capacitance

$$FOM = \frac{Q}{(C_0/C_m)} \tag{12}$$

### III. SIMULATION

The simulation has been carried out in the CoventorWare software. MemMech solver is used for the piezoelectric physics. The electrode materials has been used for the simulation are platinum, tungsten, molybdenum, aluminum. A combine configuration of bottom layer of aluminum and top layer of tungsten has been simulated. The thickness of top and bottom electrodes has been taken as 150nm and piezoelectric layer (AlN) thickness of 1 $\mu$ m.

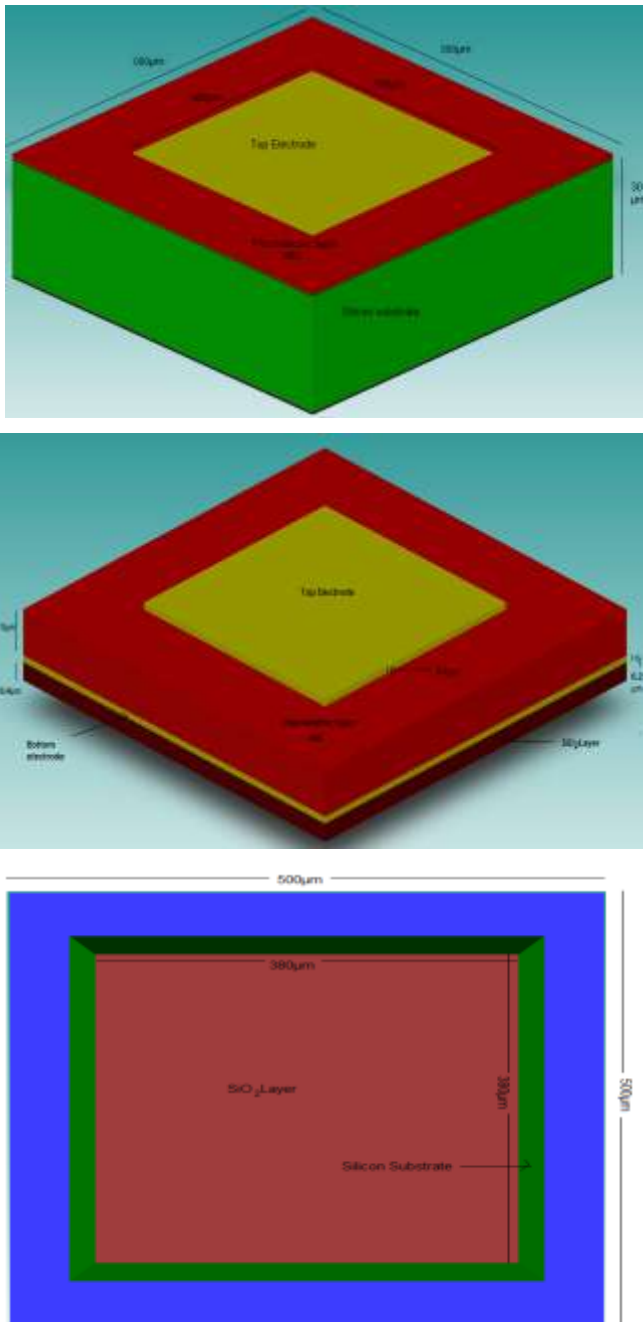


Figure 4 FBAR model, a) cross section full view b) active device layers c) bottom view of device

Figure 4(a) shows the cross section dimension of FBAR having  $500 \times 500 \mu\text{m}^2$  of all layers except top layer which has cross section area of  $300 \times 300 \mu\text{m}^2$ . Figure 4(b) shows the top four layers thicknesses which have top electrode, aluminium nitrite layer, bottom electrode and the support layer (silicon oxide). Figure 4(c) shows the back side etched part dimensions.

Simulation has been carried by applying 1V DC supply to the top electrode for the capacitance and the maximum displacement. The capacitance ( $C_0$ ) of the sandwiched

configuration is shown in the table III and the displacement is shown in the figure 5.

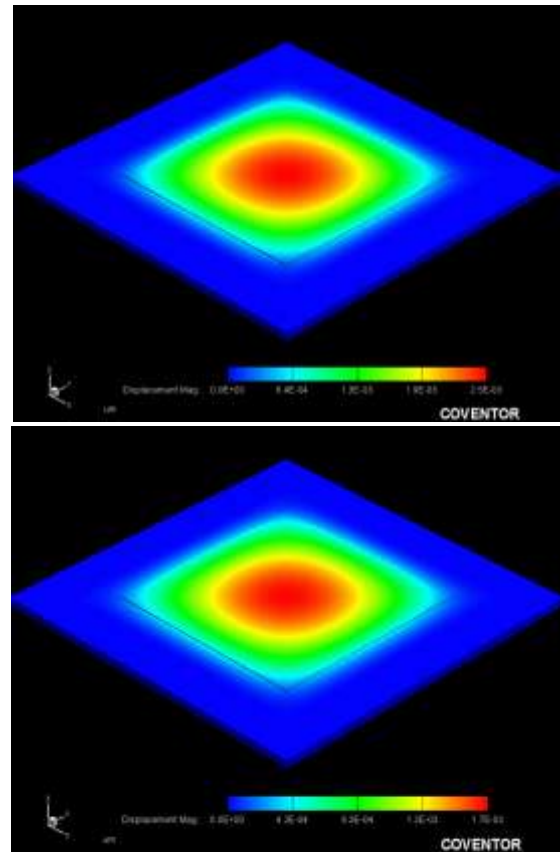
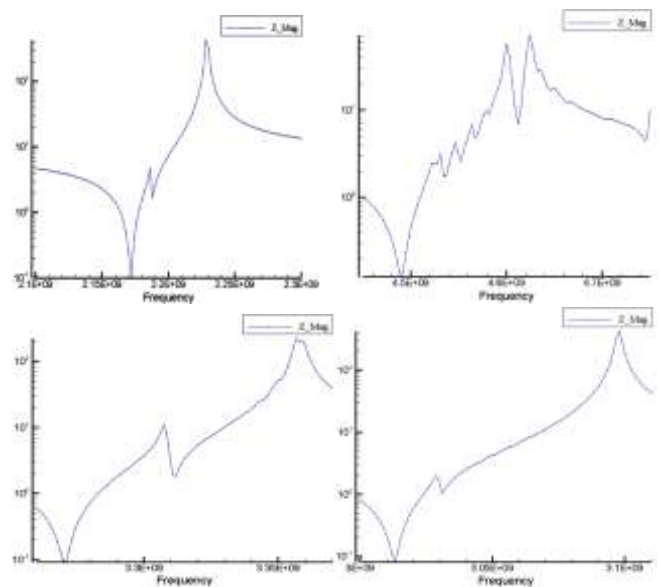


Figure 5 (a) Displacement in platinum electrode FBAR (b) Displacement in aluminium electrode FBAR



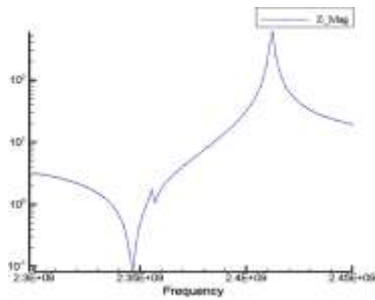


Figure 6 Impedance curve (a) Platinum (b) Aluminium (c) Tungsten and Aluminium (d) Molybdenum (e) Tungsten

For the model analysis, the harmonic supply of 1V has been given to the top electrode. The resonant frequencies, quality factors and impedance responses have been obtained. The impedances are shown in the figure 6.

#### IV. RESULT AND DISCUSSION

The device with piezoelectric layer (AlN) thickness of 1µm and top and bottom electrode with 150 nm has simulated and the quality factor and effective coupling coefficient has been extracted. The quality factor and coupling coefficient are shown in the figure 7 and 8 respectively with respect to the resonant frequencies.

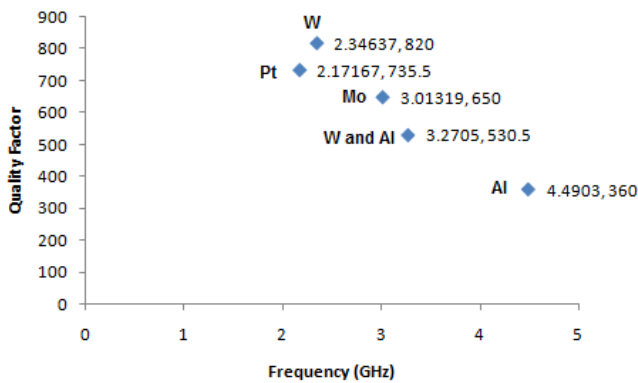


Figure 7 Quality factors

The resonant frequencies have been obtained for the platinum and tungsten as 2.17 GHz and 2.34 GHz respectively which are almost half in comparison to the aluminum resonant frequency of 4.49 GHz. Whereas, molybdenum and mixed electrodes configuration (W and Al) have their resonant frequency at 3.01 GHz and 3.27 GHz respectively. The lowest resonant frequencies have been obtained for Pt and W because of lower acoustic velocity and high acoustic impedance. The acoustic velocity of aluminum is much higher than other electrodes and it shows the higher resonant frequency. The maximum quality factor has been obtained for the W and Pt of 820 and 735.5 respectively whereas the aluminum has lowest

quality factor of 360. Molybdenum and mixed electrode configuration of W and Al have quality factor of 650 and 530.5 respectively. Quality factor depends on the acoustic impedance. The higher acoustic mismatch between device and outside environment is required so that the leakage of energy reduces and obtains the higher quality factor. The acoustic impedance of platinum and tungsten is much higher than aluminum. Molybdenum has intermediate value of acoustic impedance and so quality factor.

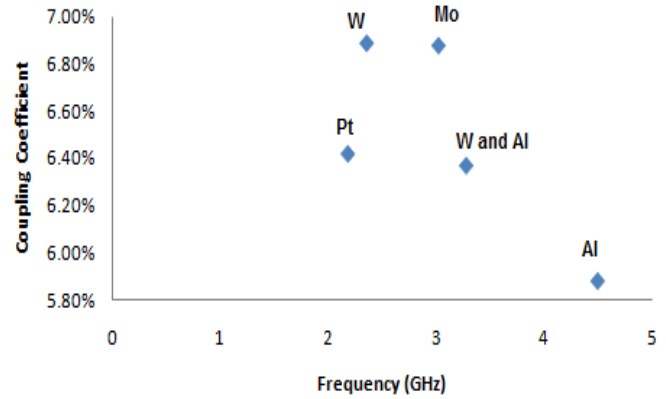


Figure 8: Effective coupling coefficient

The coupling coefficient of the molybdenum and tungsten has been obtained as 6.89% and 6.88% respectively which are highest as compared to other electrode materials. The coupling coefficient of the Pt and mixed electrode configuration of W and Al has been obtained as 6.42% and 6.37% respectively. Aluminum has lowest coupling coefficient of 5.88% and so the lowest value for the FOM.

Table III BVD parameters

AlN piezoelectric	Co (pF)	Cm (pF)	Lm (nH)	Rm (ohms)
Platinum	9.4937	0.53	10.15	0.188
Aluminum	9.4805	0.5701	2.206	0.1728
Tungsten (top) Aluminum (bottom)	9.4935	0.525	4.5	0.175
Molybdenum	9.48563	0.57	4.9	0.145
Tungsten	9.48307	0.57	7.78	0.1452

The BVD model equivalent parameters has been calculated by using the simulated result of capacitance and resonant frequencies and shown in the table III. The lowest series resistance has been obtained for molybdenum and tungsten.

## V. CONCLUSION

The film bulk acoustic resonator (FBAR) has been designed and simulated for the frequency, quality factor, coupling coefficient, impedance response and BVD parameter for the different electrode configurations. The results for different electrode materials have been compared. The higher resonant frequency has been obtained for the Al. However, Al leads to the lower coupling coefficient and the quality factor. The higher quality factor has been obtained for Pt and W. Tungsten and molybdenum have the higher coupling coefficient. FBAR has the large range of flexibility for the frequency, quality factor and coupling coefficient for different electrode materials. It suggests that materials for the electrode can be selected according to the requirement of the parameters.

## REFERENCES

- [1] R. Ruby, P. Bradley, J. Larson III, Y. Oshmyansky, and D. Figueredo, in 2001 IEEE International Solid-State Circuits Conference (IEDM) (IEEE, 2001), p. 120.
- [2] K. M. Lakin and J. S. Wang, "Acoustic bulk wave composite resonators," *Appl. Phys. Lett.* **38**, 3, 125–127, 1981
- [3] Lakin KM, Wang J, Kline G, Landin A, Chen Y, Hunt J, "Thin film resonators and filters", *Proc IEEE Ultrasonics Symp* 1982, **1**:466–475
- [4] R. C. Ruby, P. Bradley, Y. Oshmyansk, J. D. Chien, and A. Larson, "Thin film bulk wave acoustic resonators \_FBAR\_ for wireless applications", *Proc.-IEEE Ultrason. Symp.* **1**, 813–821, 2001
- [5] X. T. Qiu, R. Tang, J. Zhu et al., "Experiment and theoretical analysis of relative humidity sensor based on film bulk acoustic-wave resonator," *Sensors and Actuators B*, vol. 147, no. 2, pp. 381–384, 2010
- [6] X. Qiu, J. Zhu, J. Oiler, C. Yu, Z. Wang, and H. Yu, "Film bulk acoustic wave resonator based ultraviolet sensor," *Applied Physics Letters*, vol. 94, no. 15, Article ID 151917, 2009
- [7] M. Nirschl, A. Blüher, C. Erler et al., "Film bulk acoustic resonators for DNA and protein detection and investigation of in vitro bacterial S-layer formation," *Sensors and Actuators A*, vol. 156, no. 1, pp. 180–184, 2009
- [8] G. Sharma, L. Liljeholm, J. Enlund, J. Bjurström, I. Katardjiev, and K. Hjort, "Fabrication and characterization of a shear mode AlN solidly mounted resonator-silicone micro-fluidic system for in-liquid sensor applications," *Sensors and Actuators*, vol. 159, no. 1, pp. 111–116, 2010
- [9] R.-C. Lin, Y.-C. Chen, W.-T. Chang, C.-C. Cheng, and K.S. Kao, "Highly sensitive mass sensor using film bulk acoustic resonator," *Sensors and Actuators A*, vol. 147, no. 2, pp. 425–429, 2008
- [10] P. Curie and J. Curie, *Bull. Soc. Fr. Mineral.* **3**, 90, 1880
- [11] J. D. Larson III, P. D. Bradley, S. Wartenberg, and R. C. Ruby, "Modified Butterworth-Van Dyke circuit for FBAR resonators, and automated measurement system," *Proc.-IEEE Ultrason. Symp.* **1**, 863–868, 2000
- [12] J. Y. Park, H. C. Lee, K. H. Lee, H. M. Lee, and Y. J. Ko, "Micro-machined FBAR RF filters for advanced handset applications," in *IEEE Intl. Conf. Solid State Sensors, Actuators and Microsyst.*, pp. 911–914, Boston, MA, June 2003